Conformational Changes in Phospholipase A_2 upon Binding to Micellar Interfaces in the Absence and Presence of Competitive Inhibitors. A ^1H and ^{15}N NMR Study†

Anton R. Peters,‡ Niek Dekker,‡,§ Lambertus van den Berg,§ Rolf Boelens,‡ Robert Kaptein,*,‡ Arend J. Slotboom,§ and Gerard H. de Haas§

Bijvoet Center for Biomolecular Research and Center for Biomembranes and Lipid Enzymology, State University of Utrecht, P.O. Box 80.054, 3584 CH Utrecht, The Netherlands

Received May 8, 1992

ABSTRACT: An NMR study has been made of porcine pancreatic phospholipase A_2 (PLA) in three environments: free in solution, in a binary complex with dodecylphosphocholine micelles, and in a ternary complex with a micelle and the substrate-like inhibitor (*R*)-1-octyl-2-(*N*-dodecanoylamino)-2-deoxyglycero-3-phosphoglycol. ^1H and ^{15}N chemical shifts, amide exchange rates, and NOE intensities are compared for the enzyme in different environments. From these data, structural differences are found for the N-terminal part, the end of the surface loop at residues Tyr69 and Thr70, and the active site residue His48, and also for the Ca-binding loop (residues 28–32). Specifically, when binding to a micelle, the side chains of residues Ala1, Trp3, and Tyr69, as well as all protons of Thr70, are found to be closer together. After subsequent introduction of the competitive inhibitor, further changes are found for these residues. The N-terminus is flexible in PLA free in solution, in contrast with the crystal structures where it adopts an α-helical conformation. According to the NMR data, this helix is rigidly formed only in the ternary complex. Furthermore, in the ternary complex, the N-terminal amino group and the exchangeable hydrogen at N3 of the ring of His48 are observed. We propose that PLA is activated in two steps. An initial conformational change occurs upon binding to a micellar interface. The catalytically active conformation of the enzyme, which has an extensive network of hydrogen bonds, is formed only when binding a substrate or competitive inhibitor at a lipid–water interface.

Phospholipase A_2 (PLA)[1] is a calcium-dependent enzyme that stereospecifically cleaves the 2-acyl linkage of phosphoglycerides (Waite, 1987). The crystal structures have been determined for the enzymes from porcine and bovine pancreas (Dijkstra et al., 1981, 1983) and from the venom of the rattlesnake *Crotalus atrox* (Brunie et al., 1985), as well as for the secretory phospholipase from synovial fluid (Wery et al., 1991). A mechanism of catalysis resembling that of serine proteases has been proposed on the basis of biochemical data and the crystal structure (Verheij et al., 1980). In all structures, the active center residues His48 and Asp99 are located in a cavity which is surrounded by a wall consisting of hydrophobic residues.

It is well known that PLA has only a low activity toward substrate present as monomers. When the substrate is present in aggregated form such as in micelles, the enzyme is up to four orders of magnitude more active. Several possibilities have been suggested to explain this interfacial activation process [for a review, see Volwerk and de Haas (1982); also see Jain and Berg (1989) and Scott et al. (1990a)]. In so-called enzyme models (Verger & de Haas, 1976; Verheij et al., 1981), the protein itself is thought to become activated when binding at an interface. In one such model, Verger and de Haas suggested that the enzyme has a distinct interface recognition site (IRS) with which it interacts with the micelle. The enzyme would become activated at an interface by a change in conformation, resulting in an increased rate of hydrolysis. By contrast, in substrate models it is proposed that in an interface the substrate would have a conformation or orientation which facilitates diffusion into, and degradation by, the enzyme. Also, when coming from the interface instead of from water, dehydration of the substrate and the enzyme at the interface has already been accomplished. This would enhance hydrophobic interactions and facilitate diffusion of the substrate into the enzyme as well. Evidence has been found that dehydration does occur (Van Scharrenburg et al., 1985; Jain & Vaz, 1987; Jain et al., 1988).

These different explanations are not mutually exclusive. The subject has been addressed by X-ray studies on PLA complexed with inhibitors [Thunnissen et al. (1990), for porcine pancreatic PLA; White et al. (1990), for cobra venom PLA; Scott et al. (1990b), for bee venom PLA]. From these studies, a picture has emerged that PLA is a rigid enzyme and that interfacial activation is basically due to the environment of the substrate. Recently, however, structures for PLA from synovial fluid in the absence and presence of an inhibitor were reported (Scott et al., 1991). The N-terminal helix of uncomplexed PLA is shifted with respect to the other known structures and with respect to the inhibitor-bound form. Similarly, for a fungal lipase, a large change of conformation occurs when binding an inhibitor: a helix was found to move,

† These investigations were carried out under the auspices of the Netherlands Foundation for Chemical Research (SON) with financial support from the Netherlands Organization for Scientific Research (NWO) and from the Bridge Programme of the European Community (nr. BIOT-0194).

* Address correspondence to this author.

‡ Bijvoet Center for Biomolecular Research.

§ Center for Biomembranes and Lipid Enzymology.

[1] Abbreviations: 1D, one dimensional; 2D, two dimensional; 3D, three dimensional; CIDNP, chemically induced dynamical nuclear polarization; DPC, fully deuterated *n*-dodecylphosphocholine; HMQC, heteronuclear multiple-quantum correlation; inhibitor, (*R*)-1-octyl-2-(*N*-dodecanoylamino)-2-deoxyglycero-3-phosphoglycol; IRS, interface recognition site; NOE, nuclear Overhauser effect; PLA, porcine pancreatic phospholipase A_2; TOCSY, total correlation spectroscopy.

0006-2960/92/0431-10024$03.00/0

uncovering the active site (Brady et al., 1990; Brzozowski et al., 1991).

Our aim is to use high-resolution NMR spectroscopy to obtain detailed information about the structure of the ternary complex consisting of protein bound to a micelle and containing a single inhibitor molecule in its active site. The assignment of the ^1H and ^{15}N resonacnes of PLA free in solution has been reported (Fisher et al., 1989; Dekker et al., 1991a). Previous NMR studies have shown that inhibitors bind in a 1:1 stoichiometry to the protein under micellar conditions, and specific protein–inhibitor interactions could be identified (Dekker et al., 1991b). Here we present NMR data of PLA in different environments, indicating that the structure of PLA free in solution is not as rigid as suggested by the crystallographic studies. Conformational changes occur upon binding to a micelle, but the enzyme assumes its catalytically competent conformation only in a ternary complex with micelles and a substrate analogue.

MATERIALS AND METHODS

Protein. Native porcine pancreatic and ^{15}N-labeled PLA were isolated as reported before (Nieuwenhuizen et al., 1984; Dekker et al., 1991a).

Fully Deuterated DPC. Fully deuterated dodecylphosphocholine was obtained from Cambridge Isotope Laboratories.

Inhibitors. The synthesis of (*R*)-1-octyl-2-(*N*-dodecanoylamino)-2-deoxyglycero-3-phosphoglycol and (*R*)-2-(*N*-dodecanoylamino)hexanol-1-phosphoglycol have been described by Dijkman et al. (1990).

Sample Preparation. The NMR samples typically contained 1 mM enzyme in either 93% H_2O/7% D_2O or 99.96% D_2O, always containing 50 mM $CaCl_2$ and 150 mM NaCl. The pH was adjusted to 4.3 or 5.0 (uncorrected meter reading), and the temperature was 313 K. In the ternary complex, the ratio PLA:DPC was ca. 1:100, and the inhibitor was present in slight excess to PLA. For the D_2O samples, all exchangeable protons were replaced by deuterons as described before (Dekker et al., 1991b).

For the D_2O exchange experiments, ^{15}N-labeled PLA lyophilized from H_2O/salt buffer was dissolved in D_2O (3 mM), and measurements were started within 6 min. For the titration discussed below, the sample originally had a concentration of 4 mM ^{15}N-labeled PLA, but, upon addition of 87 equiv of DPC and 1.2 equiv of inhibitor, it was diluted to 2.4 mM. For the 3D NOE-HMQC spectrum, a sample was prepared containing 3.2 mM [^{15}N]PLA, 3.9 mM inhibitor, and 263 mM DPC (1:1.2:82) in H_2O/salt at pH 5.0.

NMR Spectroscopy. All NMR spectra were recorded on Bruker AM 600 and AMX 500 spectrometers (the former at the SON hf-NMR facility, Department of Biophysical Chemistry, Nijmegen University, The Netherlands). Two-dimensional NOE spectra were recorded at 600 MHz with a 32-step phase cycle with mixing times in the range of 25–200 ms.

The ^{15}N–^1H HMQC spectra (Müller, 1979) were recorded with a refocusing delay of 4 ms. The spectra for the exchange experiments consisted of 128 × 2K data points, each record obtained by adding 8 (solution) or 12 (ternary complex) transients; these experiments had a duration of about a half hour. For the study of PLA free in solution, 7 spectra were recorded in a period of 21.9 h; for the study of the ternary complex, 40 spectra were recorded in 20.9 h. The ^{15}N spectral width was 56 ppm, centered on the amide resonances. The spectra of the titration were recorded with a wide ^{15}N spectral range of 137 ppm. In this case, 256 records of 2K data points with 24 transients each were recorded.

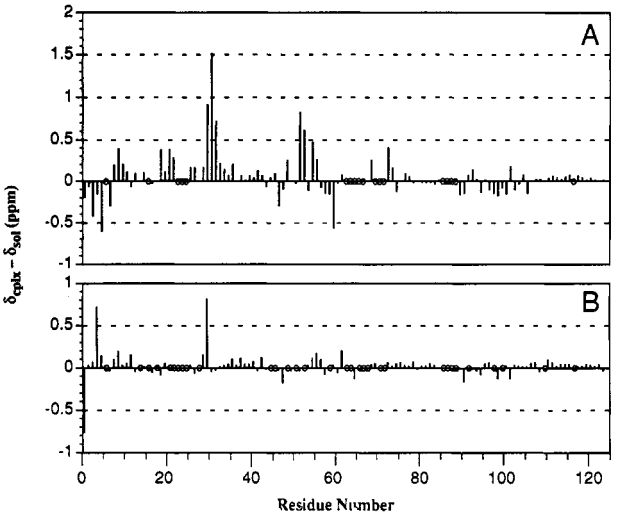

FIGURE 1: Chemical shift changes. The changes in chemical shift of the ternary complex with respect to uncomplexed PLA are plotted. If data at pH 5.0 are not available, those from spectra at pH 4.3 are used (refer to the supplementary material). When data are missing, an "o" is plotted. (Panel A) amide protons. (Panel B) Cα protons.

The 3D NOE-HMQC spectrum was recorded essentially as before (Dekker et al., 1991a) with 200 × 82 × 1024 data points (^1H, ^{15}N, ^1H) with 16 transients per record and a phase cycle of 16 steps.

Processing. For the 3D spectrum, the t_1 and t_2 domains were extended with about 50% by linear prediction (Olejniczak & Eaton, 1990). Further processing of the 2D and 3D spectra was essentially as described before.

Assignments. The assignments obtained for PLA free in solution (Fisher et al., 1989; Dekker et al., 1991a) were transferred to the spectra of the PLA/DPC and ternary PLA/inhibitor/DPC complexes by monitoring chemical shift changes during titration and identifying patterns in the various NOE spectra. For the backbone protons, the assignments could be checked and extended using the 3D spectrum.

RESULTS

Chemical Shifts. For the PLA/inhibitor/DPC complex, backbone assignments could be made for 103 of the 124 residues (14 other amides have been observed, but their NOEs did not allow sequential assignment). For the assigned protons, the changes in chemical shift of PLA under various conditions could be investigated. The differences in chemical shift between the ternary complex and the free protein for backbone protons are graphically presented in Figure 1. Note that large shift changes occur not only for residues involved in inhibitor binding (these were identified in the X-ray studies), but also for residues in the N-terminal part. An extensive shift table, including data for side chain protons as well, is available in the supplementary material.

HMQC Experiments. Figure 2 shows the ^1H–^{15}N HMQC spectra of PLA recorded during the titration with DPC and inhibitor. Panel A shows the spectrum of 4 mM PLA in H_2O solution. Some resonances are indicated for comparison with the subsequent spectra.

First, 1.5 equiv DPC was added (6 mM). Under these conditions, the PLA is about 90% saturated with monomeric DPC since the K_d is ca. 0.3 mM (Van Dam-Mieras et al., 1975). Most of the remainder of the DPC is present in micelles (critical micelle concentration = 1.1 mM), but the concentration of micelles is low (ca. 30 μM). Therefore, most of the

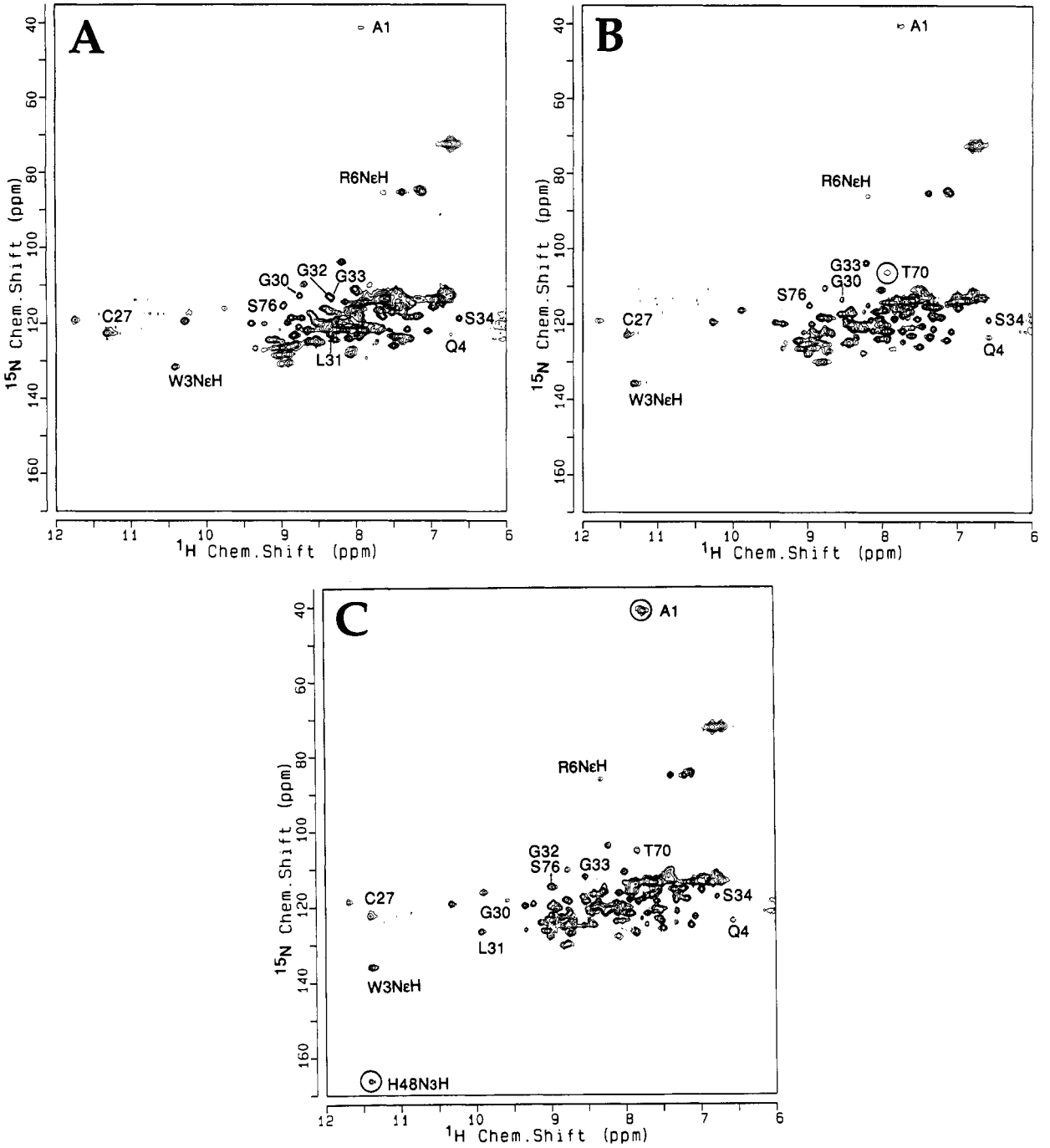

FIGURE 2: 500-MHz ^1H–^{15}N HMQC spectra of porcine pancreatic PLA. Conditions: 313 K, pH 5.0, 50 mM $CaCl_2$, 150 mM NaCl. (Panel A) 4.0 mM PLA. (Panel B) 2.6 mM PLA, 226 mM DPC (1:87). (Panel C) 2.4 mM PLA, 2.9 mM inhibitor I1, 211 mM DPC (1:1.2:87). Contours are plotted at the same levels for all spectra. Levels increase exponentially with a factor of 2. Some resonances which show large changes in chemical shift or intensity are identified. The resonance of Ser76 does not move much but is indicated because it overlaps with that of Gly32 in panel C. Three new resonances are circled in panels B and C.

PLA is not bound to micelles. The HMQC spectrum, which shows only amide protons (mainly in the backbone) does not change much. For side-chain protons, some shifts can be observed in NOE spectra of a similar sample. Residues involved are Phe5, Ile9, Phe22, Leu41, His48, Tyr52, Phe63, Tyr69, Phe106, and Tyr111. These residues are part of the substrate-binding pocket at the interior of the protein, and the shifts indicate that a DPC molecule is bound here.

In Figure 2B, 86 equiv of DPC has been added, and under these conditions PLA is fully bound to the micelles (Dekker et al., 1991b). Several residues show a large change in chemical shift. Examples are the indole proton of Trp3, which is at the IRS [shifts from $\delta(^1H/^{15}N)$ = (10.4/132) ppm to (11.3/136) ppm]; Arg6 NεH; and Gly33 backbone amide. Furthermore, the signal of Thr70, which was not observable under the previous conditions, now appears in the spectrum (circled).

In Figure 2C, 1.2 equiv of inhibitor has been added. Besides further changes in shifts (see Figure 1), a new cross peak can be observed, and another increases in intensity (circled). The cross peak at (11.4/167) ppm is due to the exchangeable proton on N3 in the ring of His48. This assignment is based on the observation of strong NOEs to the His48 C2 and C4 protons. In the crystal structures, there is a hydrogen bond between the active center residues His48(N3) and a carboxylate oxygen of Asp[99]. Apparently, due to inhibitor binding the exchange rate is lowered such that the hydrogen can be observed in the

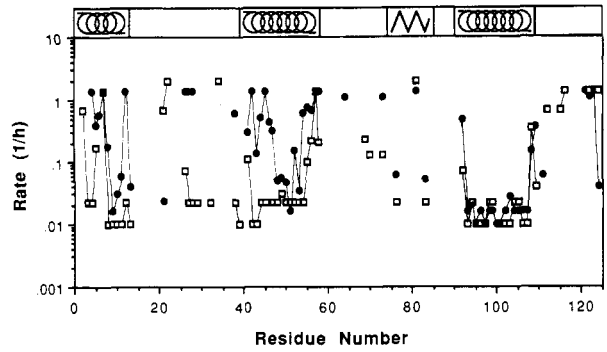

FIGURE 3: Backbone amide exchange rates. Filled circles (●) refer to uncomplexed PLA, open squares (□) to the ternary PLA/inhibitor/DPC complex. Sequential residues for which a value could be determined are connected by a line. Values at the top and bottom ranges are lower and upper bounds, respectively. The helical and β-sheet regions are indicated. Most of the amides for which no data are shown are exchanging fast (rate > 2 h^{-1}), but some amides have not been assigned, and no data are available.

spectrum, presumably because of fixation of the hydrogen bond.

In the 2D NOE spectra of this complex in water, there is a proton resonating at 10.56 ppm. Since it does not give a signal in the ^1H–^{15}N HMQC spectra, it is not a ^{15}N-labeled protein amide proton. It has a strong NOE to the His48 C2 proton, and a weak one to the C4 proton, and therefore is assigned to the amide proton in the inhibitor, which is hydrogen bonded to His48(N1). This shows that the inhibitor is bound to the active center.

The resonance at (7.7/42) ppm is due to the N-terminal amino group of Ala1, as can be deduced from the ^{15}N chemical shift and from intraresidue and sequential NOEs (data not shown). The cross peak of this amino group is weakly visible in all spectra, but when the inhibitor is added, the resonance sharpens and its integrated intensity increases by a factor of about 4. This increase in intensity must be due to slowing down of the exchange with water.

Exchange Rates. Figure 3 shows the exchange rates of all backbone amides that could be observed immediately after dissolving PLA in D_2O. The data for free PLA have been presented earlier (Dekker et al., 1991a) and are included in Figure 3 for comparison with the data obtained for the ternary PLA/inhibitor/DPC complex. In general, the exchange rates are higher for the free protein than for the ternary complex, indicating that the former is more flexible. Numerical values are listed in the supplementary material.

NOE Data. For PLA in water solution, and for the PLA/inhibitor/DPC complex, quantitative NOE data are available from buildup series in H_2O and D_2O. For the PLA/DPC complex, an NOE spectrum in D_2O is available which can be compared with a corresponding spectrum of the same sample to which the inhibitor (*R*)-2-(dodecanoylamino)hexanol-1-phosphoglycol has been added. In Table I a list of selected NOEs is presented for the three conditions (PLA free in solution, PLA complexed with a micelle, and PLA complexed with a micelle and an inhibitor). It can be noted that significant changes in NOE intensities are induced both by micelle binding and by the subsequent binding of the inhibitor. These changes involve residues Ala1, Leu2, Trp3 and Phe5 (N-terminal helix), Tyr69 and Thr70 (surface loop), and His48 and Tyr52 (active center). Global inspection of the 2D NOE spectra for the various conditions show that no other significant changes of the structure do occur.

Table I: NOE Intensities[a]

proton 1	proton 2	NOE (soln)	NOE (micelle)	NOE (complex)
Ala1 (N)	Ala1 (β)	–	–	s
	Leu2 (N)	–	–	vw
Ala1 (β)	Trp3 (N)	m		–
	Trp3 (Nϵ)	m		w
	Trp3 (2)	m	w	w
	Trp3 (4)	–	vw	w
	Trp3 (5)	–	m	m
	Trp3 (6)	–	m	m
	Trp3 (7)	–	m	s
	Gln4 (N)	–		m
	Phe5 (N)	–		w
	Thr70 (α)	–	m	s
	Thr70 (β)	–	w	w
	Thr70 (γ)	–	w	w
Leu2 (N)	Trp3 (N)	w		x
Leu2 (α)	Trp3 (N)	–		w
	Trp3 (2)	w		–
Leu2 (δ_a)	Tyr69 (2,6)	m	x	s
	Tyr69 (3,5)	w	x	m
Leu2 (δ_b)	His48 (2)	–	–	m
	Tyr52 (3,5)	vw	–	m
	Tyr69 (3,5)	w	x	s
Trp3 (N)	Gln4 (N)	w		s
Trp3 ($\beta_{1,2}$)	Phe5 (N)	–		vw
Trp3 (4)	Phe5 (N)	x		s
	Ser7 ($\beta_{1,2}$)	w		–
	Thr70 (α)	x	–	w
	Tyr70 (β)	–	vw	w
	Thr70 (γ)	–	–	w
Trp3 (5)	Thr70 (α)	–	x	m
	Thr70 (β)	m	m	vw
Trp3 (6)	Thr70 (α)	–	m	s
	Thr70 (β)	–	m	m
	Thr70 (γ)	–	x	m
Trp3 (7)	Thr70 (β)	–	w	w
	Thr70 (γ)	–	x	m
Gln4 (N)	Phe5 (N)	w		m
Phe5 (β_a)	Tyr69 (2,6)	m	–	x
Phe5 (2,6)	His48 (2)	–	–	m
Phe5 (3,5)	His48 (2)	–	–	m
Phe5 (4)	His48 (2)	–	–	w
Leu31 ($\delta_{1,2}$)	Tyr69 (2,6)		–	m
	Tyr69 (3,5)		–	s
His48 (2)	Tyr52 (2,6)	–	–	vw
	Tyr69 (2,6)	–	–	vw
Tyr52 (2,6)	Tyr69 (2,6)	–	–	w
	Tyr69 (3,5)	–	m	w
Tyr52 (3,5)	Tyr69 (β_b)	vw	–	–
	Tyr69 (2,6)	–	–	m
	Tyr69 (3,5)	w	w	m
Tyr69 (N)	Tyr69 (2,6)	w		s
	Thr70 (γ)	–		w
Tyr69 (2,6)	Thr70 (γ)	–	x	m
Tyr69 (3,5)	Thr70 (α)		m	–

[a] Blank, no data available; –, definitively absent; x, NOEs overlap, no data. Qualitative estimates: vw, very weak; w, weak; m, medium; s, strong.

DISCUSSION

Uncomplexed PLA. Although an analysis of the NOE data shows that the overall structure of PLA free in solution is very similar to the crystal structure, there are important local differences. Whereas in the crystal structures the first few N-terminal residues are present in a stable α-helical conformation, they appear to be flexible in solution. The NMR data indicate a conformational equilibrium in which the helix is formed only part of the time. This we deduce from the following observations:

(1) The amide exchange rates of Gln4, Phe5 (both hydrogen bonded to the Ala1 carbonyl in the crystal structure), Arg6, Ser7, and Met8 are rather high when compared to those of

subsequent residues (9–13) or with those of the stable helix 92–109 (see Figure 3).

(2) NOEs which are typical for an α-helix are weak or absent for the first six residues. For instance, all observed sequential d_{NN} contacts are weak, and the $d_{\beta N}(i,i+3)$ NOE between Ala1 and Gln4 is absent.

(3) In addition, the amino group of Ala1 is only weakly visible, which indicates it is not fully fixed by hydrogen bonds as in the crystal structure.

(4) Furthermore, the surface loop around residues Tyr69 and Tyr70 is probably flexible. In solution, the only observed interactions of this segment with the rest of the protein are two NOEs between the aromatic ring of Tyr69 with the ring of Tyr52 and with a β-proton of Phe5. By comparison, in the ternary complex there are additional contacts with the N-terminus and the interior of the protein.

PLA–Micelle Complex. There are small changes in chemical shifts observed during titration with DPC under essentially monomeric conditions, for instance, for residues Phe5, Ile9, Phe22, and Phe106. These show that DPC is binding in the substrate pocket of the protein, which is consistent with the results of an europium luminescence study (Van Scharrenburg et al., 1985). As deduced from the chemical shifts, the effect on the protein conformation is minor.

More pronounced changes are apparent when the enzyme is fully bound to micelles. The CIDNP experiments (Dekker et al., 1991b) as well as fluorescence studies (Jain & Vaz, 1987) have shown that Trp3 interacts with the micelle. There are large changes in chemical shift of the Trp3 indole proton (+0.9 ppm) and of the Ala1 methyl group (–1.1 ppm), and there are changes in their mutual NOEs. The amide proton of Thr70 is observable now (Figure 2B; see the supplementary material for a discussion of its assignment), and the aliphatic protons have interactions with Ala1 and Trp3. In addition, Tyr69 has more NOEs with Tyr52, and several other changes in the NOE patterns and intensities can be observed (see Table I), indicating conformational changes. Apparently, a conformational transition occurs in which the side chains of the N-terminal residues Ala1, Leu2, and Trp3, and residues Tyr69 and Thr70, and Tyr52 in the active site move closer together.

PLA–Inhibitor–Micelle Complex. In the spectrum of the ternary complex, we can clearly see the resonance of the N-terminal amino group (Figure 2C). This is rarely observed with NMR, and it indicates that the amino group is involved in the extensive hydrogen-bonding network, including residues in the active center, as observed in the crystal structure (Dijkstra et al., 1983). In solution or micellar environment, this feature may be present as a minor conformation (Figure 2A,B). Upon binding of micelle and inhibitor, there are pronounced changes in the chemical shift of the backbone atoms in the N-terminal region (see Figure 1), which are likely to be due to a conformational change: the N-terminal part of the molecule adopts its helical conformation in the ternary complex. The following data contrast with those of the free enzyme, discussed above:

(1) The exchange rates of the amide protons of Gln4, Phe5, and Met8 are low, which would be in agreement with a helical conformation stabilized by hydrogen bonds involving these protons.

(2) There are sequential d_{NN} contacts between Trp3 and Gln4, and between Gln4 and Phe5 (the one between Leu2 and Trp3 could not be assessed because of overlap), as well as a weak one between Ala1 and Leu2. Also, there is a fairly strong $d_{\beta N}(i,i+3)$ NOE between Ala1 and Gln4. These NOEs are characteristic of a helix.

(3) As already noted, when a competitive inhibitor binds to the enzyme, the intensity of the signal from the terminal amino group increases, indicating the amino group is hydrogen bonded and fixed in the interior of the protein.

In the ternary complex, there are also changes (as compared to the micelle complex) in the number and intensities of NOEs involving Tyr69 and Thr70. Apparently, the conformational changes initiated upon micelle binding proceed in the same general direction. Note, that an inward displacement of Tyr69 was also found in crystal studies (Renetseder et al., 1988; Thunnissen et al., 1990; White et al., 1990b; Scott et al., 1991). In the complexes, Tyr69 is fixed by a hydrogen bond between its hydroxyl group and the phosphate group of the inhibitor.

Figure 1 shows a number of changes in chemical shift for the calcium-binding loop (residues 28–32). These can be understood when assuming, as proposed by Verheij et al. (1980), that the backbone amide of Gly30 is hydrogen bonded to the carbonyl of the *sn*-2 chain of the inhibitor, which was observed in the crystal structure (Thunnissen et al., 1990). Nonetheless, we find that this particular amide proton is exchanging fast (no signal observed in the first spectrum of the exchange experiment).

Figure 3 shows that the exchange of almost all amide protons in the ternary complex is slowed down as compared to the protein free in solution, in spite of the slightly higher pH at which measurements were made. Most notably, stabilization seems to occur for the helix 40–58, and for the beginning of the first helix, although the relatively fast exchange of Ser7 is somewhat puzzling.

The N-Terminus. With respect to the N-terminus, we conclude that this region is rather flexible in solution and adopts a rigid helical conformation as observed inthe crystal structure only when the enzyme is binding a substrate analogue in the ternary complex with a micelle. It seems that crystal structures of uncomplexed pancreatic PLA's more resemble the conformation of PLA in the ternary complex than the enzyme free in solution, which according to the NMR data has more motional freedom. In the crystal structures of a PLA from synovial fluid (Scott et al., 1991), a conformational change was found as well for the N-terminal helix and for the calcium-binding loop. In the uncomplexed molecule, the entrance of the hydrophobic binding pocket is rather narrow.

The Active Site. Another set of data indicates that structural changes occur in the active site as well. In the spectra of the PLA/inhibitor/DPC complex, some new NOEs are observed, among others involving His48 at the active site. In the crystal structures, the His48 N3 ring proton is hydrogen bonded to a carboxyl oxygen of Asp99. In solution, we identified an NOE between the β-protons of Asp99 and the His48 C4 proton, indicating that these residues are near each other. However, in Figure 2A, no trace can yet be found of the hydrogen-bonded proton. Only when PLA is complexed with the micelle and when it binds the inhibitor do the His48 C2 and N3 ring protons become visible (at 6.25 and 11.42 ppm respectively) and show several NOE interactions. This probably indicates that unless a substrate analogue is bound, these resonances are broadened because the histidine ring has motional freedom. In the ternary complex this ring is better fixed, the hydrogen bond with Asp99 is possibly formed only under these conditions, and these residues are in their proper orientation for catalytic activity.

A related observation involves Tyr73. In the crystal structure, the hydroxyl proton is hydrogen bonded to Asp99,

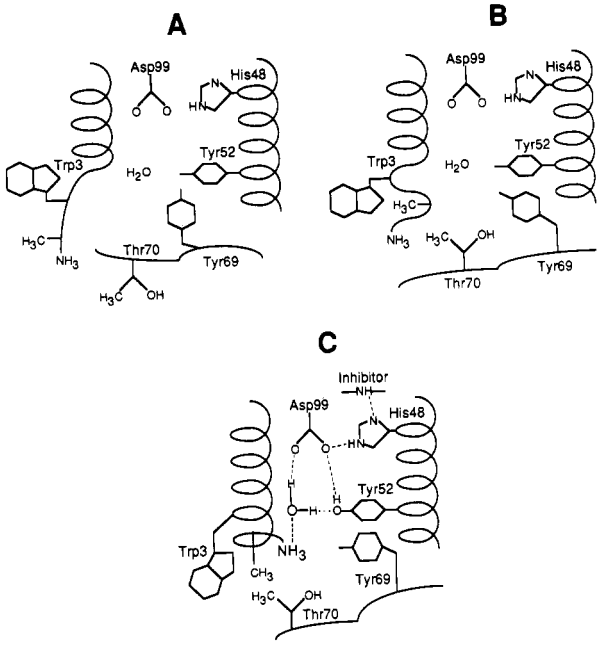

FIGURE 4: Schematic overview of structural changes in PLA. (Panel A) Conformation in solution. The N-terminus is not helical, and Thr70 has no interactions with the rest of the molecule, but Tyr69 has weak interactions with Tyr52. The internal hydrogen-bond network is incomplete. (Panel B) Conformation in a micelle. There are rearrangements in the N-terminus: the Trp3 and Ala1 side chains have interactions with the micelle. Tyr69 and Thr70 move inward. The hydrogen-bond network is incomplete. (Panel C) Conformation in a micelle with inhibitor bound. The N-terminus has a helical conformation, and the hydrogen-bond network is formed. Residues Ala1, Trp3, Tyr69, and Thr70 move. The water molecule is known from crystal structures but has not been observed in NMR spectra. For clarity, not all interactions are shown. Specifically, in the crystal structures the N-terminal amino group has hydrogen bonds with the side chain of Gln4 and the backbone of Glu71. The Tyr69 hydroxyl group is binding to the phosphate group of the inhibitor. In all three environments, there is a hydrogen bond between the side chains of Tyr73 and Asp99 (not shown).

and this exchangeable proton is visible in our spectra under all conditions studied. The resonances from the ring protons are broad but visible in solution, but they could not be identified in the spectra of the micelle-bound enzyme. For the ternary complex, four resonances are observed. The most likely explanation is that fast rotation of the aromatic ring is no longer possible in this complex, and each proton is fixed in a somewhat different environment.

CONCLUSIONS

From all these data, we conclude that neither PLA free in solution nor PLA bound at an interface is in its catalytically active conformation. Only when binding a substrate analogue is the hydrogen-bonding network formed. Furthermore, the enzyme free in solution shows flexibility, especially in the N-terminal region and surprisingly also in the active site. This contrasts with the view that emerges from the crystal structures, which suggests that a rigid structure and a catalytically competent conformation is assumed already by the free enzyme. The various states of the enzyme as deduced from the NMR data are schematically shown in Figure 4. In the enzyme free in solution, the N-terminal region and the active center do not have a rigid conformation (Figure 4A). When binding at a micelle, the side chains of Ala1, Trp3, and Thr70, as well as Tyr52 and Tyr69, are brought in closer contact (Figure 4B). Finally, when forming a ternary complex by binding a substrate analogue, additional interactions between these residues occur, but, most importantly, some crucial hydrogen bonds are formed, fixing the N-terminus and the active site residues (Figure 4C).

These results also bear upon the mechanism of interfacial activation. The crystallographic studies have favored "substrate" models, in which the substrate conformation, hydrophobic interactions, and dehydration play a role. The conformational changes within the enzyme found in this study indicate that an activation mechanism according to an "enzyme" model at least plays a role for pancreatic phospholipase A_2. It should be noted, however, that our data indicate that activation takes place in two steps as discussed above [cf. also Verheij et al. (1981)].

SUPPLEMENTARY MATERIAL AVAILABLE

Two tables listing ^1H and ^{15}N chemical shifts for the uncomplexed PLA, the PLA/micelle, and the PLA/inhibitor/micelle complexes and listing the amide exchange rates for uncomplexed PLA and the PLA/inhibitor/micelle complex (7 pages). Ordering information is given on any current masthead page.

REFERENCES

Brady, L., Brzozowski, A. M., Derewenda, Z. S., Dodson, E., Dodson, G., Tolley, S., Turkenburg, J. P., Christiansen, L., Huge-Jensen, B., Norskov, L., Thim, L., & Menge, U. (1990) *Nature 343*, 767–770.

Brunie, S., Bolin, J., Gewirth, D., & Sigler, P. B. (1985) *J. Biol. Chem. 260*, 9742–9749.

Brzozowski, A. M., Derewenda, U., Derewenda, Z. S., Dodson, G. G., Lawson, D. M., Turkenburg, J. P., Bjorkling, F., Huge-Jensen, B., Patkar, S. A., & Thim, L. (1991) *Nature 351*, 491–494.

Dekker, N., Peters, A. R., Slotboom, A. J., Boelens, R., Kaptein, R., & de Haas, G. H. (1991a) *Biochemistry 30*, 3135–3146.

Dekker, N., Peters, A. R., Slotboom, A. J., Boelens, R., Kaptein, R., Dijkman, R., & de Haas, G. H. (1991b) *Eur. J. Biochem. 199*, 601–607.

Donné-Op den Kelder, G. M., Hille, J. D. R., Dijkman, R., de Haas, G. H., & Egmond, M. R. (1981) *Biochemistry 20*, 4074–4078.

Dijkman, R., Dekker, N., & de Haas, G. H. (1990) *Biochim. Biophys. Acta 1043*, 67–74.

Dijkstra, B. W., Kalk, K. H., Hol, W. G. J., & Drenth, J. (1981) *J. Mol. Biol. 147*, 97–123.

Dijkstra, B. W., Renetseder, R., Kalk, K. H., Hol, W. G. J., & Drenth, J. (1983) *J. Mol. Biol. 168*, 163–179.

Fisher, J., Primrose, W. U., Roberts, G. C. K., Dekker, N., Boelens, R., Kaptein, R., & Slotboom, A. J. (1989) *Biochemistry 28*, 5939–5946.

Jain, M. K., & Vaz, W. L. C. (1987) *Biochim. Biophys. Acta 905*, 1–8.

Jain, M. K., & Berg, O. G. (1989) *Biochim. Biophys. Acta 1002*, 127–156.

Jain, M. K., Rogers, J., & de Haas, G. H. (1988) *Biochim. Biophys. Acta 940*, 51–62.

Müller, L. (1979) *J. Am. Chem. Soc. 101*, 4481–4484.

Nieuwenhuizen, W., Kunze, H., & de Haas, G. H. (1974) *Methods Enzymol. 32B*, 147–154.

Olejniczak, E. T., & Eaton, H. L. (1990) *J. Magn. Reson. 87*, 628–632.

Renetseder, R., Dijkstra, B. W., Huizinga, K., Kalk, K. H., & Drenth, J. (1988) *J. Mol. Biol. 200*, 181–188.

Scott, D. L., White, S. P., Otwinowski, Z., Yuan, W., Gelb, M. H., & Sigler, P. B. (1990a) *Science 250*, 1541–1546.

Scott, D. L., Otwinowski, Z., Gelb, M. H., & Sigler, P. B. (1990b) *Science 250*, 1563–1566.

Scott, D. L., White, S. P., Browning, J. L., Rosa, J. J., Gelb, M. H., & Sigler, P. B. (1991) *Science 254*, 1007–1010.

Thunnissen, M. M. G. M., AB, E., Kalk, K. H., Drenth, J., Dijkstra, B. W., Kuipers, O. P., Dijkman, R., de Haas, G. H., & Verheij, H. M. (1990) *Nature 347*, 689–691.

Van Dam-Mieras, M. C. E., Slotboom, A. J., Pieterson, W. A., & de Haas, G. H. (1975) *Biochemistry 14*, 5387–5393.

Van Scharrenburg, G. J. M., Slotboom, A. J., de Haas, G. H., Mulqueen, P., Breen, P. J., & Horrocks, W. deW., Jr. (1985) *Biochemistry 24*, 334–339.

Verger, R., & de Haas, G. H. (1976) *Annu. Rev. Biophys. Bioenerg. 5*, 77–119.

Verheij, H. M., Volwerk, J. J., Jansen, E. H. J. M., Puijk, W. C., Dijkstra, B. W., Drenth, J., & de Haas, G. H. (1980) *Biochemistry 19*, 743–750.

Verheij, H. M., Egmond, M. R., & de Haas, G. H. (1981) *Biochemistry 20*, 94–99.

Volwerk, J. J., & de Haas, G. H. (1982) in *Molecular Biology of Lipid–Protein Interactions* (Jost, P. C., & Griffith, O. H., Eds.) pp 69–150, Wiley, New York.

Waite, M. (1987) *The Phospholipases. Handbook of Lipid Research Vol. 5* (Hanahan, D. J., Ed.) Plenum Press, New York.

Wery, J.-P., Schevitz, R. W., Clawson, D. K., Bobbitt, J. L., Dow, E. R., Gamboa, G., Goodson, T., Jr., Hermann, R. B., Kramer, R. M., McClure, D. B., Mihelich, E. D., Putnam, J. E., Sharp, J. D., Stark, D. H., Teater, C., Warrick, M. W., & Jones, N. D. (1991) *Nature 352*, 79–82.

White, S. P., Scott, D. L., Otwinowski, Z., Gelb, M. H., & Sigler, P. B. (1990) *Science 250*, 1560–1563.

Registry No. PLA, 9001-84-7; DPC, 29557-51-5; (*R*)-1-octyl-2-*N*-(dodecanoylamino)-2-deoxyglycero-3-phosphoglycol, 142723-65-7.